Quantitative results near the band edges of disordered systems

E. N. Economou*

Exxon Research and Engineering Company, Annandale, New Jersey 08801

C. M. Soukoulis

Exxon Research and Engineering Company, Annandale, New Jersey 08801
and Ames Laboratory-U.S. Department of Energy and Department of Physics, Iowa State University, Ames, Iowa 50011†

M. H. Cohen

Exxon Research and Engineering Laboratory, Annandale, New Jersey 08801

A. D. Zdetsis

Department of Physics and Research Center of Crete, Heraklion, Crete, Greece
(Received 28 November 1984)

By combining the coherent-potential approximation, the potential-well analogy, and theories for the near tail in the density of states, we obtain, for the first time, explicitly quantitative results for the various quantities of interest near the band edges of disordered systems. These results exhibit a certain universality and can be expressed in terms of simple analytic functions, provided that disorder is not larger than about $\frac{1}{5}$ of the bandwidth.

I. INTRODUCTION

Recent developments based on the potential-well analogy[1-3] allow us to calculate transport or localization properties such as position of the mobilities edge E_c, localization length λ, fluctuation length ξ, conductivity σ, and the mobility[4] μ from quantities such as the mean free path l, self-energy Σ, etc., which can be obtained from mean-field theories such as the coherent-potential approximation (CPA).

Furthermore, recent[5] as well as older work[6-9] permits us to obtain the near tails in the density of states (DOS) due to bound states in *clusters* of sites. Combining these results with the CPA result for the DOS, one obtains quantitative results for the DOS in the entire energy range starting from inside the band all the way to the extreme tail due to states (if any) bound to single sites.

Thus combining the CPA, the potential-well analogy, and the results for the near tail in the DOS, one for the *first* time is in a position to obtain *explicit quantitative* results concerning the behavior near the band edges of disordered systems. Furthermore, most of these results up to disorders about $\frac{1}{5}$ of the bandwidth exhibit a quasi-universal character and can be expressed in terms of simple analytic functions. These results are obtained for a square or cubic lattice with diagonal disorder and nearest-neighbor hopping. It will be very interesting to investigate whether the universality noted above is also retained for more complicated types of disorder.

One should ask how accurate the above-mentioned results are. We can check the CPA-based results as follows:

In one dimension (1D), there is a rigorous result for the DOS and the localization length in the white-noise problem[8-10] against which our CPA-based DOS can be checked. Furthermore, it is possible to obtain numerically very accurate results for the localization length versus energy.

In two and three dimensions (2D and 3D) one can check the CPA-based results for the localization length λ (or the fluctuation length ξ) with the results of the numerical method of strips[11-13] and rods. Furthermore, the position where the tail in the DOS starts can be checked approximately from the position of the few lowest eigenvalues of energy in finite disordered systems. Finally, our recent work[14] allows us a semiquantitative check, namely that of the form of the functional dependence of our results on the disorder and the other parameters of the problem. It must be mentioned that the CPA-based results for λ, ξ, σ, and E_c at the center of the band[1,15] have already been checked successfully against the strip- or rod-method results.

II. FORMALISM

We consider a tight-binding model with diagonal disorder only

$$H = \sum_n |n\rangle \epsilon_n \langle n| + V\sum_{n,m}' |n\rangle\langle m| , \qquad (2.1)$$

where the sites $\{n\}$ form a regular lattice (square in 2D, simple cubic in 3D, and simple hypercubic in general) of lattice constant a. V is the hopping matrix element and the common probability distribution $p(\epsilon_n)$ of each ϵ_n has a variance w^2. We distinguish two classes of $p(\epsilon_n)$: (a) the terminating ones, such as the rectangular of total width W ($w^2 = W^2/12$), for which $p(\epsilon_n)=0$ when $|\epsilon_n| \gg w$, and (b) the ones with tails, such as the Gaussian, for which $p(\epsilon_n)\neq 0$ even when $|\epsilon_n| \gg w$. Off-diagonal disorder, omitted here, may create some qualita-

tively new features.

The CPA calculates the average (i.e., the arithmetic mean) Green's function corresponding to H from an effective periodic Hamiltonian resulting from (2.1) by replacing each ϵ_n by a common self-energy Σ, which is determined by the following equation:

$$\Sigma(E) = \int d\epsilon_n \, p(\epsilon_n) \frac{\epsilon_n}{1 - (\epsilon_n - \Sigma)G_0(E - \Sigma)} , \qquad (2.2)$$

where $G_0(E)$ is the diagonal element of the unperturbed Green's function in which all ϵ_n's are the same. In the one-dimensional case one can obtain the logarithmic average (i.e., the geometric mean) of G as well from a self-energy Σ_g which obeys the following equation:

$$\int d\epsilon_n p(\epsilon_n) \ln[1 - (\epsilon_n - \Sigma_g)G_0(E - \Sigma_g)] = 0 . \qquad (2.3)$$

For relatively weak disorder ($wG_0 \ll 1$) one can expand Eqs. (2.2) and (2.3) to obtain

$$\Sigma = w^2 G - (2w^4 - \mu_4)G^3 + O(w^6) , \qquad (2.4)$$

$$\Sigma_g = \tfrac{1}{2}w^2 G - (\tfrac{3}{8}w^4 - \mu_4/4)G^3 + O(w^6) , \qquad (2.5)$$

where $\mu_4 = \int d\epsilon_n \, \epsilon_n^4 p(\epsilon_n)$ is the fourth moment of the distribution and $G \equiv G_0(E - \Sigma)$ or $G \equiv G_0(E - \Sigma_g)$, respectively. The zero of energy is taken at the unperturbed lower ban edge. For the rectangular distribution $2w^4 - \mu_4 = \tfrac{1}{5}w^4$ and for the Gaussian case $2w^4 - \mu_4 = -w^4$.

It must be mentioned that for the second class of distributions (the ones with a tail) there is always a finite (but very small) probability for a very deep fluctuation of some ϵ_n [while the neighboring ϵ_n have values in the range $(-w, w)$]. Such an isolated potential well can trap an electron around it. The CPA equation (2.2) (which rigorously treats the scattering from a single site) correctly describes the extreme tail in the DOS resulting from these single-site bound states. However, the approximate form (2.4) misses completely these states which are associated with the pole of the integrand in Eq. (2.2). In the extreme tail Eq. (2.2) can be approximated by

$$\Sigma(E) \approx -i \frac{\pi}{G_0^2(E)} p(G_0^{-1}(E)) , \qquad (2.6)$$

and the corresponding extreme tail DOS (per unit volume) has the form

$$\rho(E) \approx -\frac{1}{a^d} \frac{G_0'(E)}{G_0^2(E)} p(G_0^{-1}(E)) . \qquad (2.7)$$

The combination of equations, (2.4) inside and near the band edge and Eq. (2.6) in the tail, approximate very well the numerical solution of Eq. (2.2) for not so large disorder.

Having Σ or Σ_g, one can obtain various quantities of interest as follows. The DOS is given by $-(1/\pi)\mathrm{Im}G_0(E - \Sigma(E))$. The mean free path is given by

$$l = \frac{V^{1/2}a}{2 \, | \, \mathrm{Re}\sqrt{\Sigma(E) - E} \, |} \qquad (2.8a)$$

for E near the band edge or in the tail. a is the lattice spacing. Inside the band for not so large disorders l is given by

$$l = \frac{v\hbar}{2 \, | \, \mathrm{Im}\Sigma \, |} , \qquad (2.8b)$$

where $v(E) = v_0(E - \mathrm{Re}\Sigma)$ is the average value of the velocity for that energy.[1] A more general formula covering both cases is

$$l = \frac{v_0(2Vd(1+c))}{2d(1-c^2)^{1/2}\ln | \, A + (A^2 - 1)^{1/2} \, |} , \qquad (2.9)$$

where

$$A \equiv A_1 + iA_2 = \frac{E - \Sigma}{2Vd} - 1 , \qquad (2.9a)$$

$$c = \frac{A_1}{2 \, | \, A_1 \, |}\{1 + A_1^2 + A_2^2 - [(1 + A_1^2 + A_2^2)^2 - 4A_1^2]^{1/2}\}^{1/2} , \qquad (2.9b)$$

and d is the dimensionality. The proof of the above formulas for l is based upon the equation $E - \Sigma = E(k - i/2l)$. Near the band edge $E(k) = Va^2k^2$ (where a is the lattice spacing) from which Eq. (2.8a) follows after some algebraic manipulations. Inside the band for not so large disorder $1/2l$ is very small so that

$$E(k - i/2l) = E(k) - i\hbar v/2l \qquad (2.10)$$

from which Eq. (2.8b) follows.

The CPA allows also the approximate determination of the conductivity[2] through the formula

$$\sigma \approx \sigma_0 = \frac{2e^2}{(2\pi)^d d\pi} \int dE' \, v_0(E - \Sigma - E')S_0(E - \Sigma_1 - E')$$

$$\times \frac{\Sigma_2^2}{(E'^2 + \Sigma_2^2)^2} , \qquad (2.11)$$

which for weak disorder becomes

$$\sigma_0 = \frac{2}{(2\pi)^d d} \frac{e^2}{\hbar} S(E)l(E) . \qquad (2.12a)$$

In the above formulas $S_0(E)$ is the area (length for $d = 2$ and $S = S_0 = 2$ for $d = 1$) of the surface of constant energy E in k space. In the disordered case S results from S_0 by changing the unperturbed relation $E = E(k)$ to

$$E - \mathrm{Re}\Sigma = \mathrm{Re}E(k - i/2l) .$$

Inside the band for weak disorder we obtain

$$S(E) \approx S_0(E - \mathrm{Re}\Sigma) \qquad (2.12b)$$

while near the band edge we have for $d = 3$

$$S(E) \approx \frac{4\pi}{a^2}\left[\frac{E - \mathrm{Re}\Sigma}{V} + \frac{a^2}{4l^2}\right] . \qquad (2.13)$$

Inside the band but near the band edge and for weak disorder it follows from (2.12a) that

$$S(E) \sim E^{(d-1)/2} \qquad (2.14)$$

while Eqs. (2.8a) and (2.4) give under the same circumstances

$$l(E) \sim E^{(3-d)/2} \ , \tag{2.15}$$

so that

$$\sigma_0 \sim E \tag{2.16}$$

for all d for weak disorder and inside but near the band edge. Recall that σ_0 in Eq. (2.16) is the weak scattering limit of the CPA conductivity and hence does not vanish for $d \leq 2$.

It has been shown[1-3] that almost all the results in localization theory can be obtained from an effective potential well whose depth is proportional to $S^{-1}l^{-(d+1)}$ and whose extent is proportional to l. Thus the localization length is given by[1]

$$\lambda = 2l_g \ , \quad 1D \tag{2.17}$$

$$\approx 2.72l \exp\left[\frac{Sl}{4}\right] \ , \quad 2D \tag{2.18}$$

$$\approx \frac{2.2 + 14.12\phi}{1-\phi}l \ , \quad 3D \tag{2.19}$$

where l is the mean free path, l_g is the mean free path corresponding to the logarithmic average of the Green's function G, S is the surface of constant energy, and ϕ is

$$\phi \equiv Sl^2/8.96 \ . \tag{2.20}$$

It follows from (2.20) that the mobility edge in 3D is given by the relation

$$Sl^2 = 8.96 \ . \tag{2.21}$$

As localized states correspond to bound states in the effective potential well, the states strongly fluctuating in amplitude above the mobility edge correspond to resonance states in the effective potential well with the resonance scattering length being essentially the length ξ. This analogy combined with numerical results[15] allows explicit determination of ξ and the conductivity σ:

$$\xi = \frac{24.4}{Sl}f(\phi) = 2.72l\frac{f(\phi)}{\phi} \ , \tag{2.22}$$

where

$$f(\phi) = 1 + \frac{6}{\phi(\phi-1)} \tag{2.23}$$

and

$$\sigma = \sigma_0/f(\phi) = \frac{e^2}{\hbar}\frac{0.0656}{\xi} \ . \tag{2.24}$$

From $\sigma(E)$ and the DOS one can obtain the mobility which is given by[4]

$$\mu(E) = \frac{1}{e\rho(E)}\frac{d\sigma}{dE} \ . \tag{2.25}$$

The CPA is inadequate for the near tail of the spectrum, which consists of states bound to potential fluctuations extending over more than a single site. This region has been studied extensively,[5-10] and the results are the following for 1D:

$$\rho_{NT}(E) \approx \frac{1}{\epsilon_{01}L_{01}}\frac{4}{\pi}\frac{|E|}{\epsilon_{01}}\exp\left[-\frac{8}{3}\left|\frac{E}{\epsilon_{01}}\right|^{3/2}\right] \ , \tag{2.26}$$

$$\epsilon_{01} = w^{4/3}/V^{1/3} \ , \tag{2.27}$$

$$L_{01} = w^{-2/3}V^{2/3}a \ , \tag{2.28}$$

$$\rho_{NT}(E) \approx \frac{1}{\epsilon_{02}}\frac{1}{L_{02}^2}0.120 \, |(E - E_{CPA}/\epsilon_{02})|^{0.5689}$$

$$\times \exp[-0.9311 \, |(E - E_{CPA})/\epsilon_{02}|] \ , \quad 2D \tag{2.29}$$

$$\epsilon_{02} = w^2/4\pi V \ , \tag{2.30}$$

$$L_{02} = w^{-1}Va \ . \tag{2.31}$$

For 3D, it is found in Ref. 7 that

$$\rho_{NT}(E) = \rho_{CPA}(8.96/\pi - x)3.092(8.96/\pi - x)$$

$$\times \exp[-1.504(8.96/\pi - x)^{1/2}] \ , \tag{2.32}$$

where x is given by

$$x = (E - E_{CPA})/\epsilon_{03} \ , \tag{2.33}$$

$$\epsilon_{03} = \frac{w^4}{4(4\pi)^2V^3} \ , \tag{2.34}$$

and E_{CPA} is the CPA band edge as determined from the approximate equation (2.4). In Eq. (2.32) we have chosen the reference energy at the mobility edge [which according to (2.22) is $8.96\epsilon_{03}/\pi$ above the CPA band edge] instead of the CPA band edge as was done in Ref. 7. Arguments for the validity of this choice are given in Ref. 5, in which it was also argued that the inclusion of short-range fluctuations changes the exponent in (2.32) to unity from one-half. The coefficient of x has been estimated (within uncertainties of a factor of 2 or so) in Ref. 5. Taking x_3/L^2, as defined in Ref. 5, to be equal to $6V$ (because in the tight-binding models discussed here the kinetic energy x_d/L^2 to confine the particle to a single site is $2dV$) and choosing the quantity ξ_0 to be equal to the mean free path, we find that the coefficient of x in the exponent is about $\frac{1}{6}$. We do not know how the preexponential of (2.32) changes as a result of short-range fluctuation. Accordingly we have chosen to take for the preexponential function form of ρ_{NT}/ρ_{CPA} the same form as holds for 2D, where we know it,[5,7] and we determine the coefficient from the requirement of smooth joining with the band CPA DOS. The final result is the following equation which modifies (2.32) as a result of short scale fluctuations:

$$\rho_{NTM}(E) = \rho_{CPA}(8.96/\pi - x)1.3 \exp\left[\frac{x - 8.96/\pi}{6}\right] \ . \tag{2.35}$$

It must be pointed out that in the near-tail equations (2.32) and (2.35) are not so different numerically. Equation (2.35) although more sophisticated is to some extent of questionable validity due to uncertainties in the coefficient of x in the exponent as well as the preexponential factor.

III. RESULTS

In what follows we approximate the true unperturbed Green's function by its form near the unperturbed band edge. Furthermore, we use the lowest order in w^2 in Eq. (2.4) or (2.5). These approximations are satisfactory as long as one stays in the vicinity of the band edge and the disorder is low, i.e., as long as both w and $|E|$ are small in comparison with the bandwidth. When these inequalities are violated one must use the full unperturbed Green's function and/or the full CPA [Eq. (2.2)]. To obtain a feeling of the magnitude of the errors involved in these approximations we plot in Figs. 1 and 2 results for the DOS and the mean free path in one- and three-dimensional lattices, respectively. Solid lines are based on the exact CPA equation [Eq. (2.2)], the complete unperturbed Green's function for the lattice, and Eq. (2.9) for the mean free path. The dashed curves are based on the lowest order in w^2 solution of Eq. (2.4), the approximate unperturbed Green's function appropriate for the band edge, i.e.,
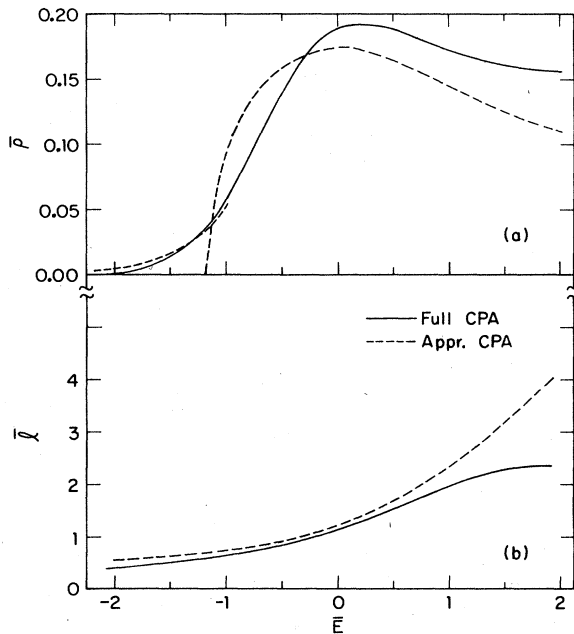

FIG. 1. (a) Density of states and (b) mean free path l for the one-dimensional case for a Gaussian distribution of standard deviation $w = 1V$. The dashed line is the approximation of the CPA valid near the band edge for weak disorder [Eqs. (2.4) and (3.1)] while the solid line is the exact CPA result [Eq. (2.2)].
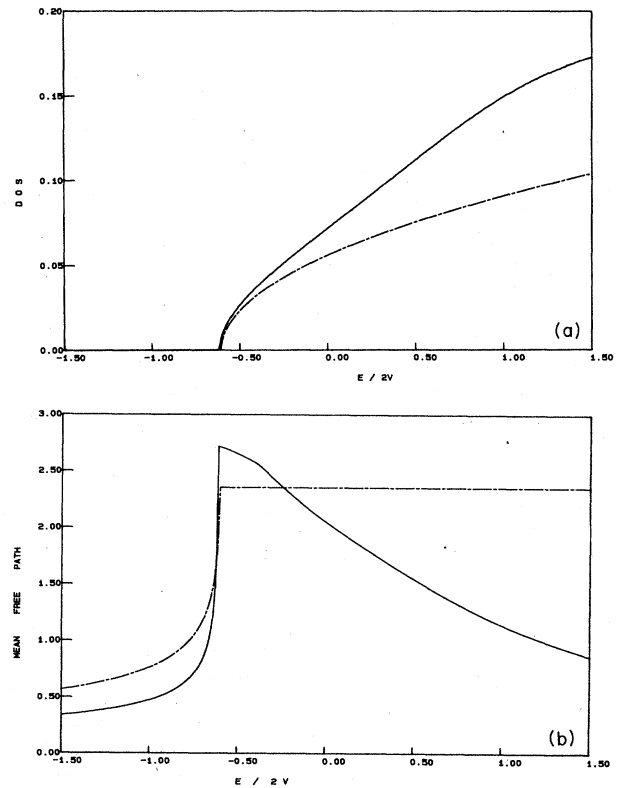

FIG. 2. (a) Density of states and (b) mean free path l for the three-dimensional case with a rectangular distribution of standard deviation $w = 2.31V$. The dashed line is the approximation of the CPA valid near the band edge for weak disorder [Eqs. (2.4) and (3.2)] while the solid line is the exact CPA results [Eq. (2.2)].

$$G_0(E) \approx \frac{-1}{\sqrt{-4VE}}, \quad 1D \tag{3.1}$$

$$G_0(E) \approx \frac{-0.2527}{V} + \frac{1}{4\pi V^{3/2}}\sqrt{-E}, \quad 3D \tag{3.2}$$

and Eq. (2.8a) for the mean free path.

Despite the fact that both $|E|/(2dV)$ and $w/(2dV)$ ($2dV$ is the unperturbed bandwidth) are not much smaller than unity, the differences between the exact and the approximate versions of the CPA are rather small, which allows us to use with confidence the approximate form of the equations. The only significant differences appear in 3D inside the band (for $E/2V \gtrsim 0.1 + E_{CPA}/2V$). The reason for that is the existence in the actual $G_0(E)$ of a Van Hove singularity at $E = 4V$ which influences the results, causing them to depart appreciably from the approximate form for relatively small energies, i.e., the DOS soon ceases to follow the square-root behavior appropriate for the band edge and appears more like a straight line. This point is very significant in analyzing optical-absorption experiments.

In what follows we use everywhere the approximate form of the equations. But one should keep in mind that

there may be significant departures when $E/|E_0-E_{VH}|$ rather than $E/(2\,dV)$ becomes comparable to unity, where $|E_0-E_{VH}|$ is the difference of the band edge E_0 from the nearest Van Hove singularity E_{VH}.

The advantage of the approximate equations is not only that they permit analytic manipulations and results, but that they produce results which exhibit a certain universality. By that we mean that most of the results depend on a single energy scale (instead of the two, w and V, originally present in the model). As a matter of fact this is a general feature of our model, independent of the CPA approximation. Indeed, it has been shown[14] rigorously that in the limit $w \ll V$ and $E \ll V$ there is a single energy (or length) scale which determines the energy dependence of most quantities of interest.

A. One-dimensional case

We examine first the 1D for which there are many exact or highly accurate independent results to serve as a check of our approximations. Furthermore, it is known that the CPA becomes more and more accurate as the dimensionality increases so the one-dimensional comparison is indeed a very severe test of the validity of our approximations.

Using for $G_0(E)$ the approximate form (3.1) and replacing it in Eq. (2.4) or (2.5) and keeping only the leading term in w^2, we obtain for Σ or Σ_g the following simple equations:

$$\Sigma^3 - E\Sigma^2 - \frac{w^4}{4V} = 0 , \tag{3.3}$$

$$\Sigma_g^3 - E\Sigma_g^2 - \frac{w^4}{16V} = 0 . \tag{3.4}$$

It is clear from the above equations that the two independent energy parameters of the problem w and V have collapsed to a single natural unit of energy ϵ_{01} as defined by Eq. (2.27). From Eq. (2.8a) it follows then immediately that there is a single natural unit of length namely L_{01} as given by Eq. (2.28). From hereon we denote by an overbar a physical quantity expressed in its natural units, e.g., $\bar{\lambda} \equiv \lambda/L_{01}$, $\bar{E} \equiv E/\epsilon_{01}$, etc. In terms of the overbar quantities we have a universal behavior, i.e., the equations for $\bar{\Sigma}$ and $\bar{\Sigma}_g$ become

$$\bar{\Sigma}^3 - \bar{E}\bar{\Sigma}^2 - \tfrac{1}{4} = 0 , \tag{3.3'}$$

$$\bar{\Sigma}_g^3 - \bar{E}\bar{\Sigma}_g^2 - \tfrac{1}{16} = 0 \tag{3.4'}$$

for any probability distribution of the disorder. This concept of the universal behavior of physical quantities near band edges is discussed in more detail in Ref. 14. The CPA DOS per unit length is

$$\bar{\rho} = \frac{1}{2\pi}\left|\mathrm{Im}\frac{1}{\sqrt{\bar{\Sigma}-\bar{E}}}\right| . \tag{3.5}$$

The CPA band edge is at $\bar{E}_B = -3/2^{4/3} \approx -1.19$, and very close to E_B, $\bar{\rho}$ becomes

$$\bar{\rho} \approx \frac{1}{2^{2/3}\sqrt{3}\pi}(\bar{E}-\bar{E}_B)^{1/2} , \quad \bar{E} \to \bar{E}_B . \tag{3.6}$$

At $\bar{E}=0$ (unperturbed band edge), $\bar{\rho}$ equals

$$\bar{\rho}(0) = \frac{\sqrt{3}}{2^{5/3}\pi} \approx 0.1737 , \tag{3.7}$$

while the exact DOS (Refs. 8 and 10) at $E=0$ is 0.1846. For $\bar{E} \gg 1$ the DOS reduces to the unperturbed one,

$$\bar{\rho}(E) \approx \frac{1}{2\pi\sqrt{\bar{E}}} , \quad \bar{E} \gg 1 . \tag{3.8}$$

The mean free path $\bar{l}$ is given by Eq. (2.8a) which takes the universal form

$$\bar{l} = \frac{1}{2}\frac{1}{|\mathrm{Re}\sqrt{\bar{\Sigma}-\bar{E}}|} \tag{2.8'}$$

and the localization length $\bar{\lambda}$ by (2.17) which becomes

$$\bar{\lambda} = \frac{1}{|\mathrm{Re}\sqrt{\bar{\Sigma}_g-\bar{E}}|} . \tag{3.9}$$

At $\bar{E}=\bar{E}_B$

$$\bar{l} = \frac{1}{2^{1/3}} \approx 0.7937 , \quad \bar{E}=\bar{E}_B \tag{3.10}$$

$$\bar{\lambda} = 2 , \quad \bar{E}=\bar{E}_B^g \tag{3.11}$$

where $\bar{E}_B^g = -\tfrac{3}{4}$ for the geometric CPA band edge in 1D. At $\bar{E}=0$

$$\bar{l} = 2^{1/3} \approx 1.26 , \quad \bar{E}=0 \tag{3.12}$$

$$\bar{\lambda} = 2^{5/3} \approx 3.1748 , \quad \bar{E}=0 \tag{3.13}$$

while the exact result for $\bar{\lambda}$ at $\bar{E}=0$ is 3.456. For $\bar{E} \gg 1$ we obtain

$$\bar{\lambda} = 4\bar{l} = 8\bar{E} , \quad \bar{E} \gg 1 . \tag{3.14}$$

The near-tail DOS has the form [Eq. (2.26)]

$$\bar{\rho}_{\mathrm{NT}} = \frac{4}{\pi}\bar{E}\exp(-\tfrac{8}{3}|\bar{E}|^{3/2}) . \tag{3.15}$$

On the other hand, the CPA tail DOS which corresponds to states localized at a single site is nonuniversal, since as it is seen from Eq. (2.7), it depends explicitly on the form of the probability distribution for ϵ_n. For Gaussian probability distribution the CPA tail DOS per unit length has the following form which is obtained by replacing in Eq. (2.7) Eq. (3.1):

$$\bar{\rho} = \frac{1}{\sqrt{2\pi}}\frac{1}{y}\frac{1}{\sqrt{-\bar{E}}}\exp\left[\frac{2}{y^{2/3}}\bar{E}\right] , \quad \bar{E} \ll \bar{E}_B \tag{3.16a}$$

$$y \equiv w/V . \tag{3.16b}$$

There are two observations. First, the combination of CPA with a Gaussian probability distribution produces an exponential DOS in the tail in the one-dimensional case (of course, for $|E| \gg V$, $\bar{\rho}$ would be Gaussian since eventually $G(E) \to -1/E$ as $E \to -\infty$). Second, this exponential (as opposed to all other results near the band edge up to now) is not universal as evidenced by the presence of the parameter y in (3.16a).

The universal part of the CPA [Eq. (3.5)] can be com-

bined with the universal near tail [Eq. (3.15)] to produce the following expression for $\bar{\rho}$:

$$\bar{\rho}_{\text{total}} = \bar{\rho} + \bar{\rho}_{\text{NT}} - \frac{2\bar{\rho}\,\bar{\rho}_{\text{NT}}}{\bar{\rho} + \bar{\rho}_{\text{NT}}} \ . \tag{3.17}$$

The interpolation form (3.17) gives a $\bar{\rho}_{\text{total}}$ which approximately equals the dominant one between $\bar{\rho}$ and $\bar{\rho}_{\text{NT}}$ and avoids to some extent the problem of double counting. At the point where $\bar{\rho}_{\text{NT}} = \bar{\rho}$, $\bar{\rho}_{\text{total}} = \bar{\rho}_{\text{NT}} = \bar{\rho}$ and as a result a spurious dip may be created around this point by (3.17). One way to avoid this is by smoothing the resulting curve $\bar{\rho}_{\text{total}}$ around this point by use of a Lorentzian-broadening function.

In Fig. 3(a) we compare our results based on (3.17) (smoothed around $\bar{E} = -0.5$) with the exact result tabulated in Ref. 14 and given by

$$\bar{\rho} = \left[\frac{2}{\pi} \right]^{1/2} \frac{N_+}{N_-^2} \ , \tag{3.18}$$

where

$$N_\pm = \int_0^\infty dt \ t^{\pm 1/2} \exp(-\tfrac{1}{6}t^3 - 2\bar{E}t) \ . \tag{3.19}$$

The agreement is very good and provides strong support for the idea that the CPA (supplemented as in the present work) provides accurate (as well as universal) description of the electronic behavior near a band edge. Equally satisfactory agreement is obtained for the localization length λ obtained from Eq. (3.5) as can be seen in Fig. 3(b), where a comparison with the exact result for λ is made. The latter is given by

$$\lambda = \frac{1}{2} \frac{N_+}{N_-} \tag{3.20}$$

where $N_\pm$ is defined in Eq. (3.19), and tabulated in Ref. 14.

In Fig. 4 we plot again the DOS per unit length analyzed into its three components: the band CPA component which exhibits universal algebraic dependence on energy, the near-tail component which has a universal form containing an exponential of energy to $\frac{3}{2}$ power, and the deep tail [not shown in Fig. 3(a)] which is not universal and (for Gaussian distribution of site energies) is exponential over a wide energy range before it becomes Gaussian for very large negative energies. The presence and shape of this third component depends on the form of the probability distribution of the site energies. For a Gaussian distribution, as the standard deviation decreases the deep tail becomes smaller and more steeply falling. For $w/V \geq 1.5$, the deep tail dominates almost the entire tail region.

B. Three-dimensional case

The successful pass of the severe one-dimensional test allows us to present now with some confidence the results of our approach for the near-band-edge region of the three-dimensional case. It must be pointed out that our results are the first detailed quantitative results in this important case.
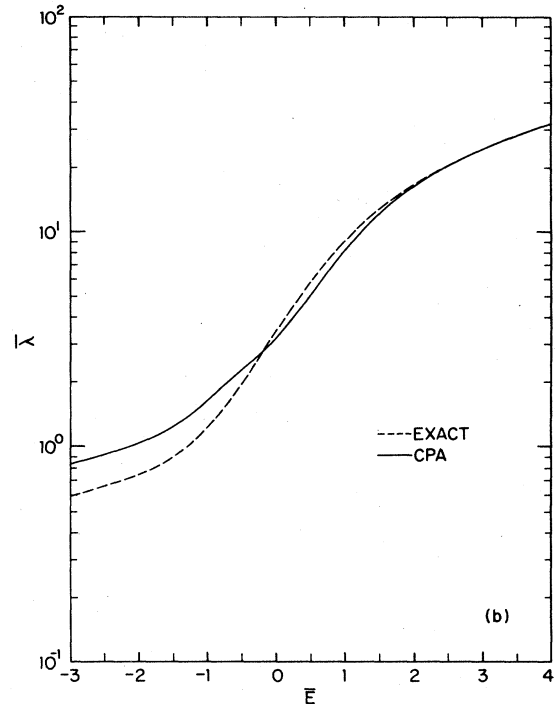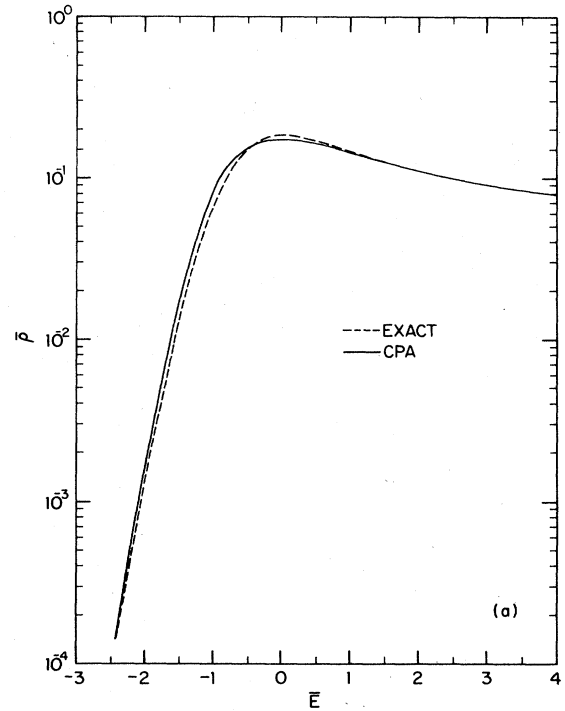

FIG. 3. (a) Density of states per unit length [in units of $(\epsilon_{01}L_{01})^{-1}$; see text] versus energy (in units of ϵ_{01}) for the one-dimensional case according to the tail supplemented CPA (solid line) and according to the exact equation [Eq. (3.18)] (dashed line). (b) Localization length λ (in units of L_{01}; see text) versus energy (in units of ϵ_{01}) for the one-dimensional case according to the tail-supplemented CPA (solid line) and according to the exact equation [Eq. (3.20)] (dashed line).
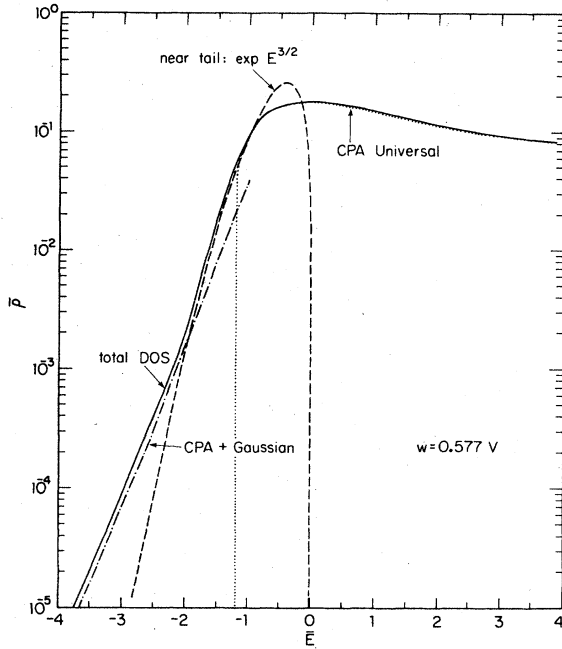
FIG. 4. Density of states per unit length (in units of $\epsilon_{01}^{-1}L_{01}^{-1}$) versus energy (in units of ϵ_{01}) for the one-dimensional case (solid line) decomposed in its three components: the band CPA (dotted line), the near tail (dashed line), and the non-universal CPA deep tail (dotted-dashed line), drawn here for the case of Gaussian disorder with standard deviation $w = 0.577V$.

In 3D we combine the general equation (2.4), which we write as follows:

$$\Sigma = w^2 G_0(E - \Sigma) - \alpha w^4 G_0^3(E - \Sigma) , \qquad (3.21)$$

where $\alpha = \frac{1}{5}$ for the rectangular distribution, and -1 for the Gaussian, with Eq. (3.2) for $G_0(E)$ to obtain the following equation for Σ:

$$\Sigma = w^2 G_0(0) + \frac{w^2}{4\pi V^{3/2}} \sqrt{\Sigma - E} - \alpha w^4 G_0^3(0) . \quad (3.22)$$

This equation reduces to a quadratic equation which can be solved easily to yield

$$\bar{E} - \bar{\Sigma} = x - 1 + 2\sqrt{-x} , \qquad (3.23)$$

where

$$x \equiv \frac{E - E_{\text{CPA}}}{\epsilon_{03}} \qquad (3.24)$$

and E_{CPA}, the CPA band edge, is given by

$$E_{\text{CPA}} = G_0(0)w^2 + w^4 \left[\frac{1}{4(4\pi)^2 V^3} - \alpha G_0^3(0) \right] . \qquad (3.25)$$

For the simple-cubic (sc) lattice $G_0(0) \approx -0.253/V$ so that

$$E_{\text{CPA}} = -0.253\frac{w^2}{V} + \left[\frac{1}{64\pi^2} + (0.253)^3\alpha \right] \frac{w^4}{V^3} . \qquad (3.26)$$

Having the self-energy $\bar{\Sigma}$ we can obtain the other quantities of interest as follows:

$$\bar{\rho} = \frac{1}{4\pi^2} | \text{Im}\sqrt{\bar{\Sigma} - \bar{E}} | , \qquad (3.27)$$

where $\bar{\rho} = \rho\epsilon_{03}L_{03}^3$ and

$$L_{03} = \frac{8\pi V^2}{w^2}a . \qquad (3.28)$$

Taking into account Eq. (3.23), we can easily show that (3.27) reduces to the free-electron form, i.e.,

$$\bar{\rho} = \frac{1}{4\pi^2}\sqrt{x} = \frac{1}{\pi^2}[(E - E_{\text{CPA}})/\epsilon_{03}]^{1/2} . \qquad (3.29)$$

The mean free path which is given by Eq. (2.8a) reduces in the present case to a constant for positive x

$$\bar{l} \equiv \frac{l}{L_{03}} = \frac{1}{2} , \quad x \geq 0 \qquad (3.30)$$

while for negative x we have

$$\bar{l} = \frac{1}{2}\frac{1}{(1 + |x| + 2\sqrt{|x|})^{1/2}} , \quad x \leq 0 . \qquad (3.31)$$

The surface of constant energy in k space is $4\pi k^2$, which, in view of the relation

$$E - \text{Re}\Sigma = \text{Re}E(k - i/2l) = V\alpha^2(k^2 - 1/4l^2) ,$$

becomes

$$S = 4\pi \left[\frac{E - \text{Re}\Sigma}{V\alpha^2} + \frac{1}{4l^2} \right] . \qquad (3.32)$$

Taking into account (3.23), we obtain

$$\bar{S} = \begin{cases} 4\pi x , & x \geq 0 \\ 0, & x < 0 \end{cases} \qquad (3.33)$$

and

$$\bar{S}\bar{l}^2 = \begin{cases} \pi x , & x \geq 0 \\ 0 , & x \leq 0 \end{cases} . \qquad (3.34)$$

The mobility edge is determined from Eq. (2.21) which is the present cases gives

$$x_c = 8.96/\pi = 2.852 \qquad (3.35)$$

or

$$(E_c - E_{\text{CPA}})/\epsilon_{03} = 2.852 . \qquad (3.35')$$

The quantity ϕ that enters in the expressions for the localization length λ [see Eq. (2.19)], the length ξ, and the conductivity σ [see Eq. (2.34)] is in the present case

$$\phi = \frac{\pi x}{8.96} = \frac{x}{x_c} . \qquad (3.36)$$

The CPA conductivity σ_0 is given by Eq. (2.11), which in the present case reduces to

$$\bar{\sigma}_0 = \begin{cases} \frac{2}{3\pi^3}4x \int_{-\infty}^{x-1} dt(x - 1 - t)^{3/2}\frac{1}{(t^2 + 4x)^2} , & x \geq 0 \\ 0 , & x < 0 . \end{cases} \qquad (3.37)$$

The integral can be performed analytically and gives

$$\bar{\sigma}_0 = \begin{cases} \dfrac{1}{6\pi^2}x \ , & x \geq 0 \\ 0 \ , & x \leq 0 \end{cases}$$

(3.38)

which is identical to the result of the weak scattering theory, namely

$$\sigma_0 = \frac{1}{12\pi^3}\frac{e^2}{\hbar}Sl = \frac{e^2}{\hbar L_{03}}\frac{1}{6\pi^2}x \ .$$

(3.38')

As it is clear from Eq. (2.23) and (2.24), the slope of σ at the mobility edge is $\frac{1}{6}$ the slope of σ_0, i.e.,

$$\left[\frac{d\sigma}{dx}\right]_{x=x_c} = \frac{1}{36\pi^2} \ .$$

(3.39)

The energy E_u around which σ is close, σ_0, can be defined from the condition $\xi = l$ which leads to $\phi \approx 4.05$, or, in the present case

$$x_u = 4.05x_c = 11.55 \ ,$$

(3.40)

$$(E_u - E_{\text{CPA}})/\epsilon_{03} = 11.55 \ .$$

(3.40')

The mobility which is given by Eq. (2.25) becomes in the present case

$$\mu = \frac{eL_{03}^2}{\hbar}\frac{d\bar{\sigma}/dx}{\rho(x)} \ ,$$

(3.41)

where

$$\frac{d\sigma}{dx} = \frac{1}{6\pi^2}\frac{\phi^4 - 2\phi^3 + 19\phi^2 - 12\phi}{[\phi(\phi-1)+6]^2} \ .$$

(3.42)

The near tail in the DOS has already been discussed [see Eqs. (2.32)–(2.35)]. The deep tail due to states bound in single sites is given in general by Eq. (2.7). In the present simple-cubic case, the quantity $G_0^{-2}(E)$ follows an almost straight line for E in the range $[-3V, -0.1V]$ as can be seen in Fig. 5. This straight line is given by the equation
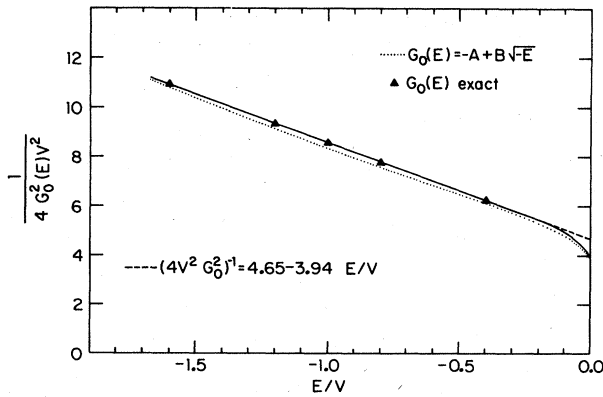
$$\frac{1}{4V^2G_0^2(E)} \approx 4.65 - 3.94\frac{E}{V} \ .$$

(3.43)

Although the particular values 4.65 and -3.94 do depend on the lattice structure, it seems that the existence of a region where $1/G_0^2(E)$ is almost a straight line is a general feature due to the existence of a point of inflection in $G_0^{-2}(E)$ which starts at $E=0$ with a square-root behavior and ends up for very negative E ($|E| \gg V$) with an E^2 behavior. Such a region of linearity of $G_0^{-2}(E)$ combined with a Gaussian probability distribution yields, according to Eq. (2.7), an exponential behavior in the DOS at the deep tail. This exponential behavior seems to be of great importance in providing an explanation for the observed features of the Urbach tail.[5,16] In the present model the deep tail due to a Gaussian is of the form

$$\bar{\rho} = \frac{16\pi}{\sqrt{2\pi}y^5}\frac{Z}{\sqrt{\beta+8.96-x}}\exp\left[-\frac{2Z}{y^2}\right], \quad x < 1$$

(3.44)

where

$$y \equiv w/V \ ,$$

(3.45)

$$\beta \equiv (4\pi)^2/y^2 \ ,$$

(3.46)

$$Z \equiv 4.65 + 3.94\frac{\beta+8.96-x}{4(4\pi)^2}y^4 \ .$$

(3.47)

Note that Eq. (3.44) is of the form $\exp(E/E_0')$ where E_0' is

$$E_0' = \frac{w^2}{7.88V}$$

(3.48)

which depends on the square of the disorder and not on the fourth power of w as does the natural unit of energy ϵ_{03}. This is not surprising since the deep tail does not follow the universal behavior characterizing the band-edge region as can be seen by the explicit y dependence of Eq. (3.44).

Note also that the various $\bar{\rho}$ obtained for different values of the disorder pass approximately through the same point $E/V = 4.65/3.94 \approx 1.18$, i.e., a focus is produced as in the usual Urbach tail.[17]

In Fig. 6 we plot the universal part of the DOS. Curve a consists of a smoothed joining of the algebraic DOS, $\bar{\rho} = (1/4\pi^2)\sqrt{x}$, with $\bar{\rho}_{\text{NT}}$ [Eq. (2.32)]. Curve b is the smoothed joining of $\bar{\rho} = \sqrt{x}/4\pi^2$ with $\bar{\rho}_{\text{NTM}}$ [Eq. (2.35)]. In Table I we tabulate these functions. It is worthwhile to points out that $\bar{\rho}_{\text{NT}}$ [Eq. (2.32)] exhibits over 2 orders of magnitude in exponential behavior as shown in Fig. 6. Of course, the modified expression $\bar{\rho}_{\text{NTM}}$ [Eq. (2.35)] exhibits by construction the exponential behavior starting from a lower value (about $x \approx -10$ as opposed to $x \approx -5$ for $\bar{\rho}_{\text{NT}}$) and falls off more steeply than $\bar{\rho}_{\text{NT}}$ although the differences are not so significant in the near tail.

In Fig. 7 we plot in logarithmic scale the two universal components of the DOS together with the deep-tail nonuniversal part. The latter is drawn for Gaussian disorder and for three different values of the standard deviation w. As w increases the deep tail starts from a higher value at $x \approx 0$ and drops faster. Below a certain point (be-
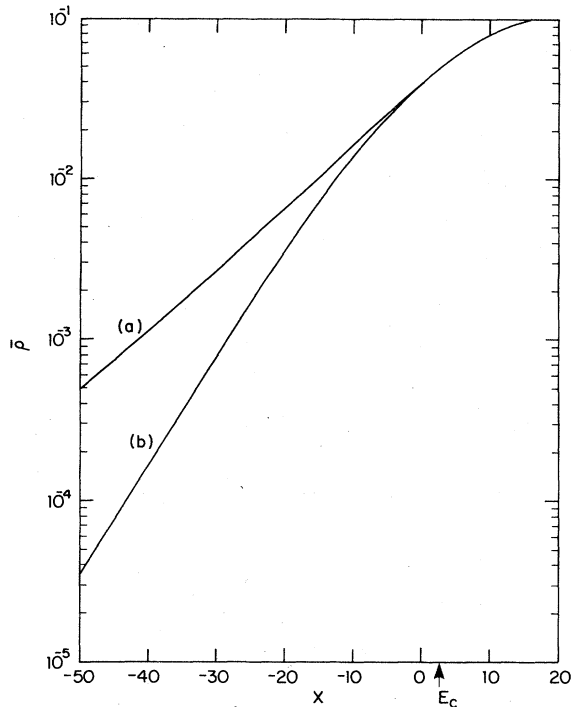
FIG. 6. (a) Density of states per unit volume (in units of $\epsilon_{03}^{-1}L_{03}^{-3}$) versus $x=(E-E_{\mathrm{CPA}})/\epsilon_{03}$ for the three-dimensional case according to the tail-supplemented CPA. The curve is the smoothed joining of Eqs. (2.32) and (3.29). (b) Density of states per unit volume (in units of $\epsilon_{03}^{-1}L_{03}^{-3}$) versus $x=(E-E_{\mathrm{CPA}})/\epsilon_{03}$ for the three-dimensional case according to the tail-supplemented CPA. The curve is the smoothed joining of Eqs. (2.35) and (3.29).
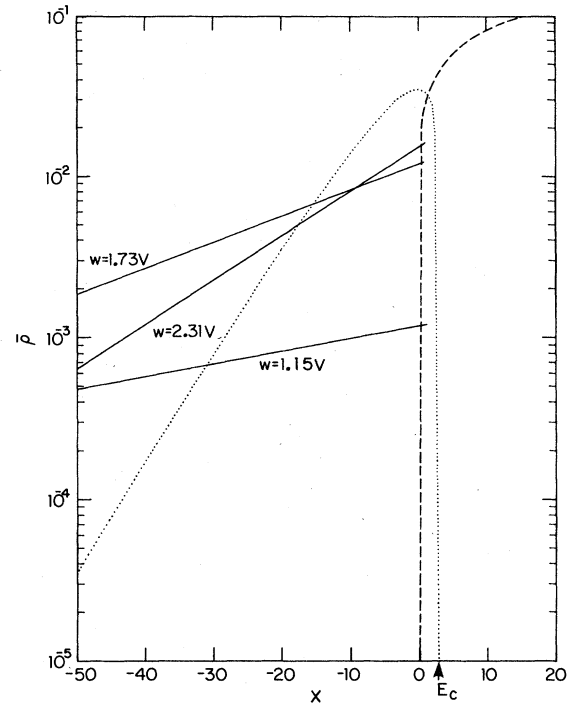

FIG. 7. Three contributions of the density of states (DOS) (in units of $\epsilon_{03}^{-1}L_{03}^{-3}$) versus $x=(E-E_{\mathrm{CPA}})/\epsilon_{03}$. The dashed line is the band CPA which equals $\sqrt{x}/4\pi^2$, the dotted line is the modified near-tail results [Eq. (2.35)] and the three solid lines give the deep-tail contribution to the DOS for Gaussian distribution with standard deviation $w/V=2.31$, 1.73, and 1.15, respectively. E_c is the mobility edge.

TABLE I. Various density of states $\bar{\rho}$ in units of $\epsilon_{03}^{-1}L_{03}^{-3}$ (for definitions see text) versus x for a three-dimensional disordered system. $x=(E-E_{\mathrm{CPA}})/\epsilon_{03}$ where E is the energy, E_{CPA} is the CPA band edge, and ϵ_{03} is a universal energy. Numbers in parentheses denote power of 10.

x	$\bar{\rho}$	$\bar{\rho}_{\mathrm{NT}}$	$\bar{\rho}_{\mathrm{NTM}}$	$\bar{\rho}_{\mathrm{CPA+NT}}$	$\bar{\rho}_{\mathrm{CPA+NTM}}$
−50	0.000	0.537(−3)	0.358(−4)	0.537(−3)	0.358(−4)
−49	0.000	0.579(−3)	0.419(−4)	0.579(−3)	0.419(−4)
−48	0.000	0.624(−3)	0.490(−4)	0.624(−3)	0.490(−4)
−47	0.000	0.674(−3)	0.573(−4)	0.674(−3)	0.573(−4)
−46	0.000	0.728(−3)	0.670(−4)	0.728(−3)	0.670(−4)
−45	0.000	0.786(−3)	0.783(−4)	0.786(−3)	0.783(−4)
−44	0.000	0.849(−3)	0.916(−4)	0.849(−3)	0.916(−4)
−43	0.000	0.918(−3)	0.107(−3)	0.918(−3)	0.107(−3)
−42	0.000	0.993(−3)	0.125(−3)	0.993(−3)	0.125(−3)
−41	0.000	0.108(−2)	0.146(−3)	0.108(−2)	0.146(−3)
−40	0.000	0.116(−2)	0.171(−3)	0.116(−2)	0.171(−3)
−39	0.000	0.126(−2)	0.199(−3)	0.126(−2)	0.199(−3)
−38	0.000	0.137(−2)	0.232(−3)	0.137(−2)	0.232(−3)
−37	0.000	0.148(−2)	0.271(−3)	0.148(−2)	0.271(−3)
−36	0.000	0.161(−2)	0.316(−3)	0.161(−2)	0.316(−3)
−35	0.000	0.175(−2)	0.369(−3)	0.175(−2)	0.369(−3)
−34	0.000	0.190(−2)	0.430(−3)	0.190(−2)	0.430(−3)
−33	0.000	0.206(−2)	0.501(−3)	0.206(−2)	0.501(−3)
−32	0.000	0.224(−2)	0.583(−3)	0.224(−2)	0.583(−3)
−31	0.000	0.244(−2)	0.679(−3)	0.244(−2)	0.679(−3)
−30	0.000	0.266(−2)	0.791(−3)	0.266(−2)	0.791(−3)
−29	0.000	0.290(−2)	0.920(−3)	0.290(−2)	0.920(−3)
−28	0.000	0.316(−2)	0.107(−2)	0.316(−2)	0.107(−2)
−27	0.000	0.345(−2)	0.124(−2)	0.345(−2)	0.124(−2)

TABLE I. (Continued).

x	$\bar{\rho}$	$\bar{\rho}_{NT}$	$\bar{\rho}_{NTM}$	$\bar{\rho}_{CPA+NT}$	$\bar{\rho}_{CPA+NTM}$
−26	0.000	0.376(−2)	0.144(−2)	0.376(−2)	0.144(−2)
−25	0.000	0.411(−2)	0.168(−2)	0.411(−2)	0.168(−2)
−24	0.000	0.449(−2)	0.194(−2)	0.449(−2)	0.194(−2)
−23	0.000	0.492(−2)	0.225(−2)	0.492(−2)	0.225(−2)
−22	0.000	0.538(−2)	0.261(−2)	0.538(−2)	0.261(−2)
−21	0.000	0.589(−2)	0.302(−2)	0.589(−2)	0.302(−2)
−20	0.000	0.645(−2)	0.349(−2)	0.645(−2)	0.349(−2)
−19	0.000	0.708(−2)	0.403(−2)	0.708(−2)	0.403(−2)
−18	0.000	0.776(−2)	0.465(−2)	0.776(−2)	0.465(−2)
−17	0.000	0.852(−2)	0.536(−2)	0.852(−2)	0.536(−2)
−15	0.000	0.935(−2)	0.618(−2)	0.935(−2)	0.618(−2)
−14	0.000	0.103(−1)	0.710(−2)	0.103(−1)	0.710(−2)
−13	0.000	0.113(−1)	0.815(−2)	0.113(−1)	0.815(−2)
−13	0.000	0.124(−1)	0.934(−2)	0.124(−1)	0.934(−2)
−12	0.000	0.136(−1)	0.107(−1)	0.136(−1)	0.107(−1)
−11	0.000	0.150(−1)	0.122(−1)	0.150(−1)	0.122(−1)
−10	0.000	0.164(−1)	0.139(−1)	0.164(−1)	0.139(−1)
−9	0.000	0.180(−1)	0.157(−1)	0.180(−1)	0.157(−1)
−8	0.000	0.197(−1)	0.178(−1)	0.197(−1)	0.178(−1)
−7	0.000	0.216(−1)	0.200(−1)	0.216(−1)	0.200(−1)
−6	0.000	0.235(−1)	0.224(−1)	0.235(−1)	0.224(−1)
−5	0.000	0.255(−1)	0.249(−1)	0.255(−1)	0.249(−1)
−4	0.000	0.274(−1)	0.275(−1)	0.274(−1)	0.275(−1)
−3	0.000	0.292(−1)	0.300(−1)	0.298(−1)	0.298(−1)
−2	0.000	0.305(−1)	0.323(−1)	0.325(−1)	0.325(−1)
−1	0.000	0.309(−1)	0.340(−1)	0.365(−1)	0.365(−1)
0	0.000	0.298(−1)	0.346(−1)	0.390(−1)	0.390(−1)
1	0.253(−1)	0.255(−1)	0.329(−1)	0.425(−1)	0.425(−1)
2	0.358(−1)	0.154(−1)	0.264(−1)	0.465(−1)	0.465(−1)
3	0.439(−1)	0.000	0.000	0.500(−1)	0.500(−1)
4	0.507(−1)	0.000	0.000	0.520(−1)	0.520(−1)
5	0.566(−1)	0.000	0.000	0.566(−1)	0.566(−1)
6	0.620(−1)	0.000	0.000	0.620(−1)	0.620(−1)
7	0.670(−1)	0.000	0.000	0.670(−1)	0.670(−1)
8	0.716(−1)	0.000	0.000	0.716(−1)	0.716(−1)
9	0.760(−1)	0.000	0.000	0.760(−1)	0.760(−1)
10	0.801(−1)	0.000	0.000	0.801(−1)	0.801(−1)

tween $x = -15$ to -20 in Fig. 7) the deep tail dominates over the near tail. Note that as the disorder decreases the region of dominance of the near tail actually shrinks because our unit of energy in Fig. 7, ϵ_{03}, decreases very fast (as w^4) with the disorder. Thus, it is only for substantial disorders (w of the order of $1V$ or larger) where the universal near-tail part plays a substantial role. Otherwise we pass from the algebraic CPA DOS to the exponential tail DOS characteristic of Gaussian disorder over a very narrow energy range. The significance of these observations for analyzing the Urbach tail in ordered and disordered materials will be analyzed in a separate publication.

Thouless and Elzain[18] have calculated the DOS for the two-dimensional tight-binding model with diagonal disorder. The CPA is used at high energies and the fluctuation theories are used at low energies, as in our approach. They have also compared their analytic results with numerical results of the DOS for the two-dimensional tight-binding model and found good agreement.

In Fig. 8 we summarize the behavior of the main quantities of physical interest near the band region of a disordered system. All these quantities have been expressed in their natural units and are plotted versus $x = (E - E_{CPA})/\epsilon_{03}$. The density of states is tabulated in Table I and is given by Eq. (3.29) for $x \gtrsim 0$ and by Eq. (2.32) or (2.35) for $-10 \lesssim x \lesssim 0$. The conductivity starts from the mobility edge with a slope of $1/36\pi^2$ and approaches asymptotically the CPA conductivity $\sigma_0 = x/6\pi^2$. The microscopic mobility starts with a discontinuity equal to $1/9(x_c)^{1/2}$, rises to a maximum and falls for large values of x as $\frac{2}{3}\sqrt{x}$. Note that the critical exponents of σ and μ near the mobility edge must be larger or equal to 1 and 0, respectively.[4] The present approach, which is equivalent in this respect to the scaling method or to the field theoretical approach, predicts the limiting values for the critical exponent. The mean free
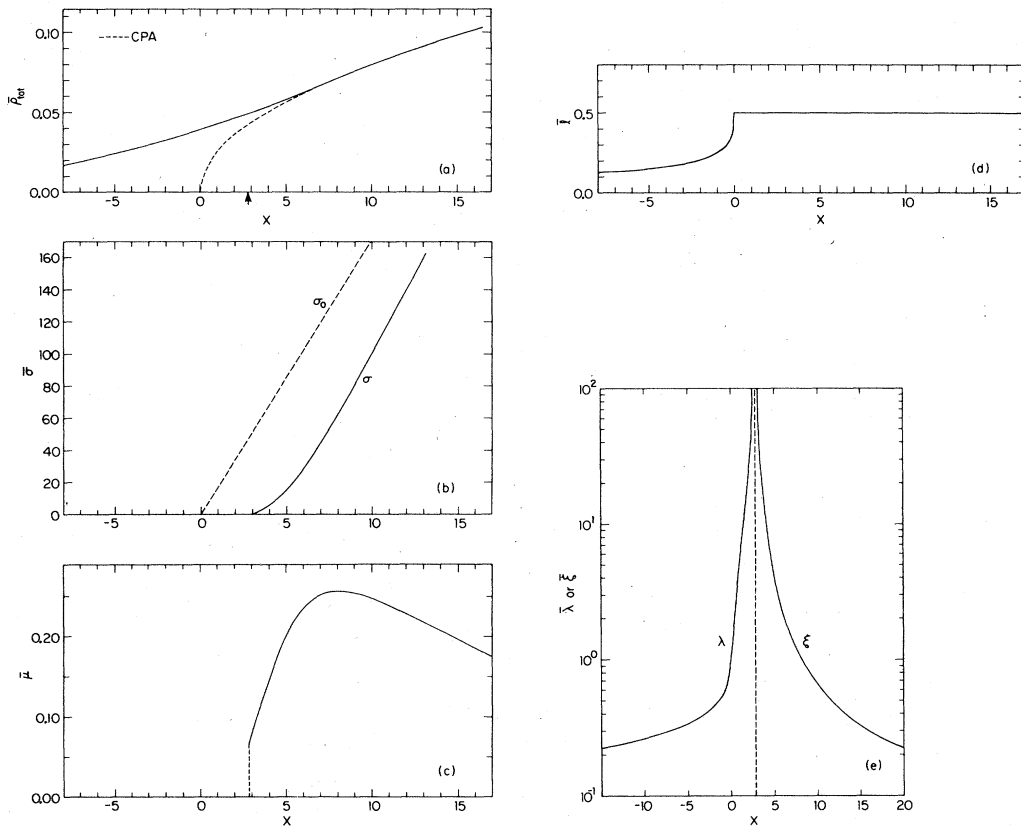
FIG. 8. Density of states $\bar{\rho}$ [panel (a), in units of $\epsilon_{03}^{-1}L_{03}^{-3}$], conductivity $\bar{\sigma}$ [panel (b), in units of $10^{-3}e^2/\hbar L_{03}$], microscopic mobility $\bar{\mu}$ [panel (c), in units of $eL_{03}^2/\hbar$], mean free path [panel (d), in units of L_{03}], localization length and correlation length ξ [panel (e), in units of L_{03}] versus $x = (E - E_{CPA})/\epsilon_{03}$.

TABLE II. Conductivity $\bar{\sigma}$, microscopic mobility $\bar{\mu}$, mean free path $\bar{l}$, localization length $\bar{\lambda}$, and correlation length $\bar{\xi}$ versus $x = (E - E_{CPA})/\epsilon_{03}$. For a plot of these functions versus x see Fig. 8.

x	$\bar{\sigma}$	$\bar{\mu}$	$\bar{l}$	$\bar{\lambda}$	$\bar{\xi}$
-10	0.000	0.000	0.120	0.264	
-9	0.000	0.000	0.125	0.275	
-8	0.000	0.000	0.131	0.287	
-7	0.000	0.000	0.137	0.302	
-6	0.000	0.000	0.145	0.319	
-5	0.000	0.000	0.155	0.340	
-4	0.000	0.000	0.167	0.367	
-3	0.000	0.000	0.183	0.403	
-2	0.000	0.000	0.207	0.456	
-1	0.000	0.000	0.250	0.550	
-0	0.000	0.000	0.500	0.110×10^1	
1	0.000	0.000	0.500	0.547×10^2	
2	0.000	0.000	0.500	0.201×10^2	
2.852	0.000	0.658×10^{-1}	0.500	∞	∞
3	0.457×10^{-3}	0.766×10^{-1}	0.500		0.144×10^3
4	0.581×10^{-2}	0.146	0.500		0.431×10^2
5	0.152×10^{-1}	0.200	0.500		0.431×10^1
6	0.283×10^{-1}	0.235	0.500		0.232×10^1
7	0.441×10^{-1}	0.252	0.500		0.149×10^1
8	0.618×10^{-1}	0.257	0.500		0.106×10^1
9	0.808×10^{-1}	0.254	0.500		0.813
10	0.100	0.247	0.500		0.654

TABLE II. (Continued).

x	$\bar{\sigma}$	$\bar{\mu}$	$\bar{l}$	$\bar{\lambda}$	$\bar{\xi}$
11	0.120	0.238	0.500		0.546
12	0.140	0.228	0.500		0.468
13	0.160	0.218	0.500		0.409
14	0.180	0.209	0.500		0.364
15	0.200	0.200	0.500		0.328
16	0.219	0.192	0.500		0.299
17	0.239	0.184	0.500		0.275
18	0.258	0.178	0.500		0.255
19	0.277	0.171	0.500		0.237
20	0.298	0.166	0.500		0.222

path remains constant down to $x=0$ and then falls off slowly according to Eq. (3.31) for $x<0$. This nonanalytical behavior at $x=0$ is a spurious result due to the CPA approximation. Finally the localization length λ and the fluctuation length ξ are of the order of L_{03} or less except close to the mobility edge where both blow up with the same critical exponent,[1,12] and the same residue, i.e.,

$$\bar{\lambda} \approx \frac{22.46}{x_c - x} \quad \text{and} \quad \bar{\xi} \approx \frac{22.46}{x - x_c} \quad \text{as } x \rightarrow x_c \ . \qquad (3.49)$$

In Table II we tabulate the values of $\bar{\sigma}, \bar{\mu}, \bar{l}, \bar{\lambda},$ and $\bar{\xi}$.

IV. SUMMARY

The combination of CPA, the potential-well analogy, and theories for the near tail in the DOS, allows us for the first time to obtain explicit results for the various quantities of interest near the band edge of three-dimensional disordered systems. For not so large $|E|$ and not so large disorder these results exhibit a certain universality as shown in Fig. 8 and in Tables I and II.

It is an interesting question for further examination whether this universality is retained in the presence of complicating factors such as off-diagonal disorder, more than one orbital per site, topological disorder, etc.

ACKNOWLEDGMENTS

*Permanent address: Department of Physics and Research Center of Crete, Heraklion, Crete, Greece.

†Present address.

[1]E. N. Economou and C. M. Soukoulis, Phys. Rev. B **28**, 1093 (1983); E. N. Economou, C. M. Soukoulis, and A. D. Zdetsis, ibid. **30**, 1686 (1984).

[2]E. N. Economou, Green's Functions in Quantum Physics, 2nd ed. (Springer, Heidelberg, 1983).

[3]E. N. Economou, Phys. Rev. B (to be published).

[4]M. H. Cohen, E. N. Economou, and C. M. Soukoulis, Phys. Rev. B **30**, (1984).

[5]C. M. Soukoulis, M. H. Cohen, and E. N. Economou, Phys. Rev. Lett. **53**, 616 (1984).

[6]J. L. Cardy, J. Phys. C **11**, L321 (1978).

[7]E. Brezin and G. Parisi, J. Phys. C **13**, L307 (1980).

[8]B. I. Halperin and M. Lax, Phys. Rev. **148**, 722 (1966); **153**, 802 (1967).

[9]J. Ziman, Models of Disorder (Cambridge University Press, Cambridge, England, 1979).

[10]B. Derrida and E. Gardner, J. Phys. (Paris) **45**, 1283 (1984).

[11]J. L. Pichard and G. Sarma, J. Phys. C **14** L127 (1981); **14**, L617 (1981).

[12]A. MacKinnon and B. Kramer, Phys. Rev. Lett. **47**, 1546 (1981); **49**, 695 (1982); Z. Phys. B **53**, 1 (1983).

[13]A. D. Zdetsis, C. M. Soukoulis, and E. N. Economou (unpublished).

[14]M. H. Cohen, E. N. Economou, and C. M. Soukoulis (unpublished).

[15]E. N. Economou, C. M. Soukoulis, and A. D. Zdetsis, Phys. Rev. B (to be published).

[16]H. Sumi and Y. Toyozawa, J. Phys. Soc. Jpn. **31**, 342 (1971); S. Abe and Y. Toyozawa, ibid. **50**, 2185 (1981).

[17]G. D. Cody, The Optical Absorption Edge of a-Si:H$_x$ in Amorphous Silicon Hydride, Semiconductors, and Semimetal, edited by J. Pankove (Academic, New York, 1984), Vol. 21B, p. 11, and references therein.

[18]D. J. Thouless and M. E. Elzain, J. Phys. C **11**, 3425 (1978).